

Optimization of SiC particle distribution during compositing of A356-SiC_p composites using D-optimal experiment design

Hamed Khosravi^{1,*}, Reza Eslami-Farsani², Mohsen Askari-Paykani

¹ Department of Materials Engineering, Faculty of Engineering, University of Sistan and Baluchestan, Zahedan, Iran

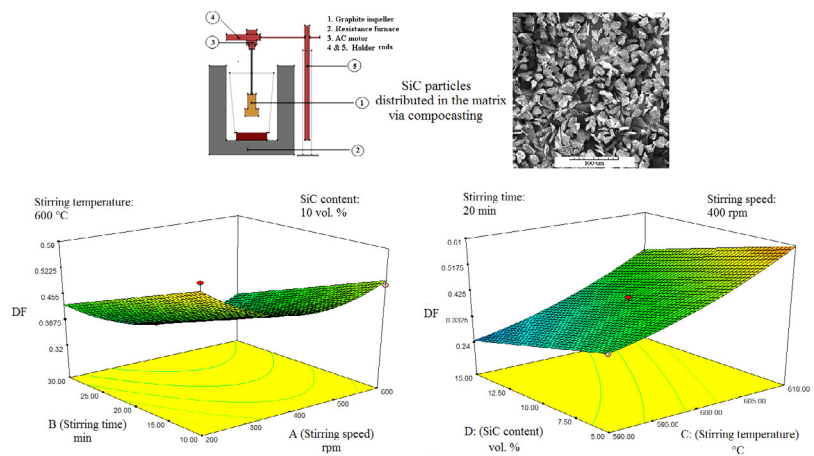
² Faculty of Materials Science and Engineering, K.N. Toosi University of Technology, Tehran, Iran

³ Department of Materials Engineering, Tarbiat Modares University, Tehran, Iran

HIGHLIGHTS

- Compositing processing of A356-SiC_p composites was studied.
- Simultaneous effects of process parameters on SiC distribution were studied.
- D-optimal design of experiment was used for optimization.

GRAPHICAL ABSTRACT



The smaller value of DF is indicative of more uniform distribution of SiC particles.

ARTICLE INFO

Article history:

Received 26 July 2017

Revised 6 December 2017

Accepted 8 December 2017

Keywords:

A356-SiC_p composite

Compositing

Optimization

Modeling

D-optimal experiment design

ABSTRACT

This paper presents an experimental design approach to the process parameter optimization for compositing of A356-SiC_p composites. Toward this end, parameters of stirring temperature, stirring time, stirring speed and SiC content were chosen and three levels of these parameters were considered. The D-optimal design of experiment (DODE) was employed for experimental design and analysis of results. In the experimental stage, different 20 μm-sized SiC particle contents (5, 10 and 15 vol %) were introduced into semisolid-state A356 aluminium alloy. Semisolid stirring was carried out at temperatures of 590, 600 and 610 °C with stirring speeds of 200, 400 and 600 rpm for 10, 20 and 30 min. The effect of these parameters on the distribution of the SiC particles within the matrix, represented by distribution factor (*DF*), was investigated. The smaller value of *DF* is indicative of the more uniform distribution of the SiC particles in the matrix. It was observed that the SiC particle content of 15 vol %, stirring temperature of 590 °C, stirring speed of 500 rpm, and stirring time of 30 min were the optimum parameter values producing the best distribution of the SiC particles in the matrix. The statistical test revealed that the main effect of the stirring temperature is the most significant factor.

* Corresponding author: Tel.: +9854-31132642 ; Fax: +9854-33447092 ; E-mail address: hkhosravi@eng.usb.ac.ir

1. Introduction

It is well known that metal matrix composites (MMCs) are characterized by high specific strength, high specific stiffness, low thermal expansion coefficient and high wear resistance [1,2]. In particular, aluminium-based MMCs have gained extensive applications in automotive and aerospace industries due to their specific characteristics. Silicon carbide (SiC) has become the main type of reinforcement used for these materials. SiC exhibits good thermal conductivity and chemical compatibility with aluminium, creating a strong bond between particle and matrix [2-5]. MMCs can be fabricated via numerous processes mainly powder metallurgy and casting techniques. The casting process is a cost effective method while powder metallurgy is costly. Among the casting techniques, stir casting is the most frequently used route for production of particulate MMCs. However, it is associated with some inherent problems arising mainly from both the apparent non-wettability of ceramic reinforcing particles by liquid aluminium alloys and the density differences between the two phases [6,7]. In order to overcome some of these drawbacks that result in non-uniform distribution of the reinforcement within the matrix alloy, extensive interfacial reactions, and formation of brittle phases at the particle/matrix interface as well as a high level of porosity new semi-solid processing techniques have been considered for manufacturing of these MMCs [8-10].

Compcasting is a semi-solid processing route in which the ceramic reinforcing particulates are added to the semi-solid matrix alloy via mechanical stirring and then cast in a mold for solidification. This technique is superior because of its simplicity, flexibility and low cost, and is considered to be the best method for preparation of large quantities of composites at low cost [11,12].

From the available literatures on MMCs, it is obvious that the size, distribution and volume fraction of the reinforcement phase as well as the matrix properties are the main factors affecting the overall mechanical and physical properties [6,7,10,11].

One of the main challenges associated with the cast MMCs is to achieve a homogeneous distribution of reinforcement within the matrix alloy. In order to achieve the optimum properties of the MMCs, the distribution of the reinforcing particles in the matrix alloy should be

uniform and the porosity levels need to be minimized. A non-homogeneous particle distribution often arises as a result of agglomeration, settling, and segregation of ceramic particles during the processing of these composite materials. The particle distribution has a significant effect on the mechanical properties of MMCs. For example, clustered particles act as crack initiation sites and have a negative influence on the mechanical properties of composite materials. Clustered particle arrangements significantly reduce the failure strain of composites. To obtain a homogeneous distribution of reinforcing particles in the cast particulate MMCs, several factors such as the good wettability of the particles with the molten alloy, proper mixing, reinforcement size, reinforcement content, mold temperature and solidification rate should be considered [10,11,13-16].

The key processing parameters affecting the final microstructure of the solidified slurry during compocasting processing are stirring time, stirring temperature and stirring speed. From an industrial point of view, it is essential to find out the best combination of compocasting parameters to attain the best mechanical and physical properties.

In general, an experiment is an observation which leads to characteristic information about a studied object [17]. One of the most common and classical approaches employed by many experimenters is one-factor-at-a-time (OFAT), in which one factor is varied while all other variables or factors in the experiment are fixed. The success of this approach depends on guesswork, luck, experience and intuition. Moreover, this type of experimentation requires large resources to obtain a limited amount of information about the process [17-21]. In many situations, in view of the high cost of experimentation, the number of observations is kept to a minimum [22-24]. With design of experiment (DOE) this number is kept as low as possible and the most informative combination of the factors is chosen [22,23]. Hence, DOE is an effective and economical solution. The aim of this so-called design is to optimize a process or system by performing each experiment and to draw conclusions about the significant behavior of the studied object from the results of the experiments. In recent years, the use of D-optimal design of experiment (DODE) in industrial experimentation has grown rapidly, due in part, to the fact that the methodology is now being introduced in standard DOE text books [19-

21], and also because facilities for constructing DODE have become generally available.

On the other hand, unlike standard classical designs, such as factorials and fractional factorials, DODE is usually not orthogonal [17,18]. This type of design is always an option regardless of the type of model the experimenter wishes to fit (for example, first order, first order plus some interactions, full quadratic, cubic, etc.) or the objective specified for the experiment (for example, screening, response surface, etc.) [18]. DODE is straight optimization based on a chosen optimality criterion and the model that will be fit. The optimality criterion used in generating DODE results in minimizing the generalized variance of the parameter estimates for a pre-specified model. As a result, the 'optimality' of a given DODE is model dependent [17,18]. That is, the experimenter must specify a model for the design before the computer can generate the specific treatment combinations. Given the total number of treatment runs for an experiment and a specified model, the computer algorithm chooses the optimal set of design runs from a candidate set of possible design treatment runs. This candidate set of treatment runs usually consists of all possible combinations of various factor levels that one wishes to use in the experiment.

Although some researchers have already utilized DOE to optimize the different types of casting routes [24], no effort has yet been made to perform this optimization on the com-casting process. In the present work, an attempt has been made to develop a model for predicting the uniformity in SiC particle within the matrix as a function of key input parameters in the com-casting processing of A356-SiC_p composites.

2. Experimental

2.1. Materials and experimental procedure

Al-A356 with a nominal chemical composition, as given in Table 1, formed the matrix and SiC particles (average size 20 μm) with 5, 10 and 15 % volume fractions were used as the reinforcement phase. A356 aluminium alloy is a hypoeutectic Al-Si alloy and its relatively broad semisolid interval (32 °C) makes it suitable for semisolid processing. The SEM micrograph of the SiC powder is shown in Figure 1. SiC particles were artificially oxidized in air at 1000 °C for 120 min to allow a layer of SiO₂ to form on them and improve

their wettability with molten aluminium. This treatment helps the incorporation of the particles while reducing undesired interfacial reactions [11].

Table 1. Chemical composition (wt %) of A356 Alloy.

Si	Mg	Mn	Zn	Cu	Fe	Al
6.93	0.38	0.23	0.26	0.25	0.11	Balance

The aluminium alloy matrix composites were synthesized by the com-casting method. Figure 2a shows a schematic representation of the com-casting apparatus used in this study. In the first stage, 1 kg of A356 aluminium alloy was put in a graphite crucible and melted at 750 °C by an electric resistance furnace. Two calibrated thermocouples were inserted into the melt and the furnace to measure their temperatures. SiC particles were preheated at 600 °C in a stainless steel crucible. Given density values for Al and SiC (2.7 and 3.2 g/cm³), the crucible charge was determined to obtain the A356-SiC_p composite samples with different SiC contents. The semi-solid stirring process was carried out by a graphite impeller (Figure 2b) [25] at temperatures of 590, 600 and 610 °C for 10, 20 and 30 min. Three different stirring speeds of 200, 400 and 600 rpm were also utilized. In the last stage, the slurry was heated up to 660 °C and stirred at this temperature for another 8 min. Casting was done in a cylindrical shaped steel mold (40 mm internal diameter and 30 mm in height), preheated at 400 °C.

The prepared samples were subjected to standard metallographic procedures and examined via an "Olympus-BX60M" light microscope.

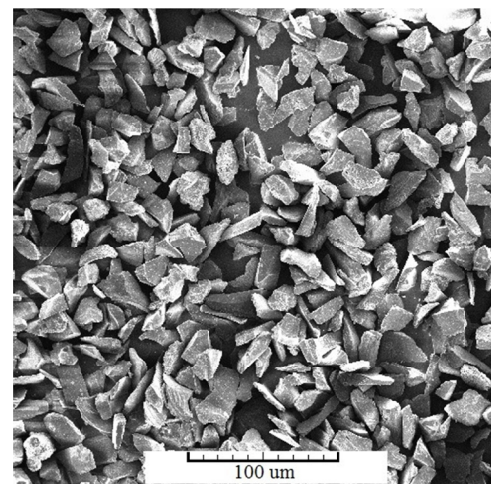


Fig. 1. SEM image of SiC particles.

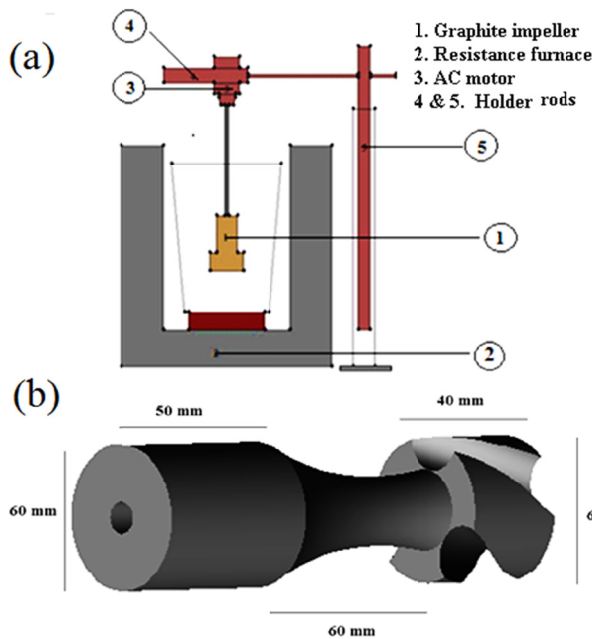


Fig. 2. (a) Schematic representation of the compocasting apparatus and (b) graphite impeller used in this study.

The distribution of the SiC particles within the matrix alloy was characterized by calculating the distribution factor (DF) defined by Eq. (1) [26].

$$DF = \frac{S.D.}{A_f} \quad (1)$$

in which A_f is the mean value of the area fraction of the SiC particles measured on 100 fields of a sample and $S.D.$ is its standard deviation. A non-uniform microscopic distribution of the reinforcing phase within a sample is reflected as a relatively high value of DF .

2.2. Experimental design and statistical analysis

To explore the effect of the operation factors on the response (DF) in the region of investigation, a DODE at three levels was performed. Stirring speed (rpm, A), stirring time (min, B), stirring temperature ($^{\circ}\text{C}$, C) and SiC content (vol %, D) were selected as independent factors. The range of values and coded levels of the factors are given in Table 2.

A polynomial equation (Eq. 2) was used to predict the response (DF , Y) as a function of independent factors and their interactions. An interaction is the failure of the one factor to produce the same effect on the response at different levels of another factor [20]. In this work, there were four independent factors; therefore, the response for the quadratic polynomials becomes:

Table 2. Independent Factors and their Levels for DODE of compocasting process.

Independent factors	Unit	level		
		-1	0	1
Stirring speed (A)	rpm	200	400	600
Stirring time (B)	min	10	20	30
Stirring temperature (C)	$^{\circ}\text{C}$	590	600	610
SiC content (D)	vol %	5	10	15

$$Y = \beta_0 + \sum \beta_i x_i + \sum \beta_{ii} x_i^2 + \sum \sum \beta_{ij} x_i x_j \quad (2)$$

where β_0 , β_i , β_{ii} , β_{ij} are the constant, linear, square and interaction regression coefficient terms, respectively, and x_i and x_j are the independent factors (A , B , C or D).

Design-Expert 7 (State-Ease, Inc., Trial version) software was used for multiple regression analysis, analysis of variance (ANOVA), and analysis of ridge maximum of data in the response surface regression (RSREG) procedure. The goodness of fit of the model was evaluated by the coefficient of determination R^2 and its statistical significance was checked by the F-test.

3. Results and discussions

This study demonstrates the effect of stirring speed, stirring time, stirring temperature and SiC content for the optimization of the compocasting route. Hence, the knowledge about the process is relatively limited, and the design is used to obtain 38 design points within the whole range of four factors for experiments. The designs and the response (DF (Y)) are given in Table 3. Following the experiments, the response surface is approximated by DODE.

The results of the DODE are presented in an ANOVA table (Table 4) with a confidence interval (CI) of 95% ($P < 0.05$) for the model. In statistics, CI is a kind of interval estimate of a population parameter and is used to indicate the reliability of an estimate. The level of confidence of CI would indicate the probability that the confidence range captures this true population parameter given a distribution of samples [17-21]. By considering a half normal plot and a normal plot (not shown here), four main effects and their squares all with $\text{CI} = 95\%$ were selected as significant factors for modeling. The effect of a factor is defined as the change in response produced by a change in the level of a factor. This

Table 3. DODE tests and the response for compocasting process.

Standard Order	Run Order	Factor 1 <i>A</i>	Factor 2 <i>B</i>	Factor 3 <i>C</i>	Factor 4 <i>D</i>	Response <i>DF</i> (by Experiment)
1	26	200	20	600	5	0.47
2	28	600	30	610	10	0.52
3	8	200	10	590	15	0.51
4	15	600	20	610	5	0.41
5	7	400	30	610	15	0.28
6	25	200	30	610	10	0.34
7	22	400	10	600	15	0.52
8	29	600	30	600	5	0.44
9	13	200	20	600	15	0.34
10	33	600	20	590	5	0.66
11	32	200	20	590	15	0.40
12	34	600	20	610	15	0.36
13	18	200	30	610	15	0.35
14	31	200	20	590	10	0.65
15	19	200	10	600	15	0.41
16	23	600	10	610	15	0.60
17	3	200	10	610	15	0.67
18	17	200	30	610	5	0.64
19	27	200	10	600	5	0.65
20	24	600	10	600	10	0.50
21	12	200	10	600	10	0.59
22	35	600	30	590	15	0.22
23	9	400	30	590	15	0.17
24	6	400	20	610	15	0.46
25	2	400	30	610	15	0.40
26	37	600	20	590	10	0.35
27	30	400	30	600	5	0.39
28	36	400	20	600	10	0.42
29	38	400	30	600	10	0.33
30	20	200	30	590	5	0.41
31	5	400	10	610	5	0.65
32	16	400	10	590	10	0.41
33	11	400	10	610	10	0.60
34	1	400	20	590	5	0.38
35	14	400	10	590	5	0.48
36	4	200	30	590	15	0.29
37	10	200	10	590	5	0.55
38	21	200	10	590	10	0.48

Table 4. ANOVA with CI = 95% for model and factors.

Source	Sum of squares	Degree of freedom	Mean square	F value	P-value Prob> F	
Model	0.60	5	0.12	281.69	<0.0001	Significant
<i>A</i>	0.019	1	0.019	45.71	<0.0001	
<i>B</i>	0.14	1	0.14	327.98	<0.0001	
<i>C</i>	0.29	1	0.29	687.10	<0.0001	
<i>D</i>	0.12	1	0.12	292.61	<0.0001	
<i>A</i> ²	0.040	1	0.040	93.53	<0.0001	
Residual	0.014	32	0.0004261			
Corrected Total	0.61	37				

is frequently called a main effect because it refers to primary factors of interest in the experiment [21].

ANOVA results for *DF* show a significant model with adequate precision of 61.818. Adequate precision compares the range of the predicted values at the design points to the average prediction error; on the other hand, adequate precision measures the signal to noise ratio and a ratio greater than 4 is desirable [18]. Here, the value of the ratio is greater than 4, so it represents an adequate model (Eq. (3)) for predicting the results within the design space without doing any further experiments.

$$Y=0.42-0.030A-0.037B+0.11C-0.069D+0.070A^2 \quad (3)$$

The quality of fittings of the equations was expressed by the coefficient of regression "Adjusted R-squared" or in a better way by "Predicted R-squared". The "Adjusted R-squared" values indicate variability in the observed response values which can be explained by the experimental factors and their interactions. The closer "Predicted R-Squared" and "Adjusted R-Squared" values are to 1, the better the fit [27]. The "Predicted R-squared" of 0.9684 is in reasonable agreement with the "Adjusted R-squared" of 0.9743. The model F-value of 281.69 implies that the model is significant ($F_{\text{model}} = 281.69 \gg F_{\text{table}}(5,32) = 2.530$) and there is only a 0.01% chance that a "Model F-value" could occur due to noise. F-value is the test for comparing the variance associated with that term with the residual variance. It is the mean square for a term divided by the mean square for the residual. This term should be as large as possible [18]. Tables of F-value (a,b) for different confidence intervals exist in statistical references [17]. Where, the first number in parenthesis is the parameter or model degree of freedom and the second one is the error's

(residuals) degree of freedom. To categorize the parameter or the model as a significant value, calculated F-value must be more than its value in the statistical tables. If the calculated value of F is greater than that in the F table at a specified probability level, a statistically significant factor or interaction is obtained [20]. The lack of fit of the F-value for the response showed that the lack of fit is not significant ($p > 0.05$) relative to the pure error. This model (Eq. (3)) can be used to navigate the design space.

The quadratic regression coefficients obtained by employing a least squares method technique to predict quadratic polynomial models for the *DF* (*Y*) are given as Eq. (3). For *Y*, the linear term and the quadratic terms (without interaction terms) of *A*, *B*, *C* and *D* were significant ($P < 0.05$).

Sum of squares (*SS*) of each factor quantifies its importance in the process and as the value of the *SS* increases the significance of the corresponding factor in the undergoing process also increases. As shown in ANOVA table (Table. 4), the effect of *C* (stirring temperature) is the strongest and then *B*, *D*, *A*² and *A*, respectively. If we consider the model equation in actual terms, one can find that the effect of *A*² and *C* is positive (synergistic effect). However, *A*, *B* and *D* have a negative (antagonism) effect on *DF*. To decrease *DF*, the positive effect should be descending and negative effect should be ascending.

Significant factors in the fitted model (Eq. (3)) were chosen as the axes for the 3D surface plots (Figures 3a and 4a) and contour plots (Figures 3b and 4b). In a contour plot (base plots in the 3D plots), curves of equal response values are drawn on a plane whose coordinates represent the levels of the independent factors. Each contour represents a specific value for the height of the

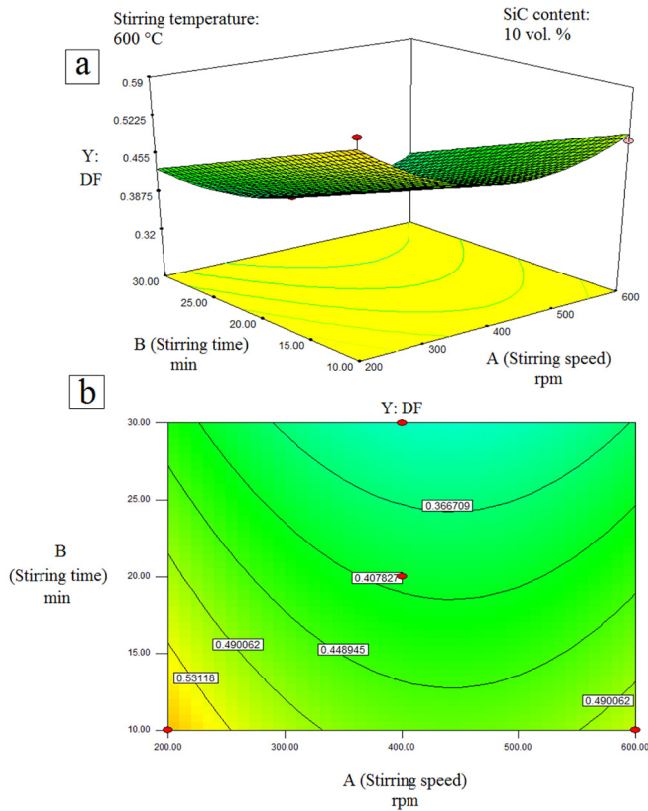


Fig. 3. a) Response surface and b) contour plots for the effect of the stirring time and stirring speed on the *DF*.

surface above the plane defined for a combination of the levels of the factors.

From Figures 3 and 4, *DF* decreases by decreasing the amount of stirring temperature and increasing the amount of SiC content and stirring time. On the other hand, the relationship between the stirring speed and *DF* was almost parabolic. This trend is in good agreement with the trend of factor effects. The observed values were reasonably close to the predicted ones as shown in Figure 5.

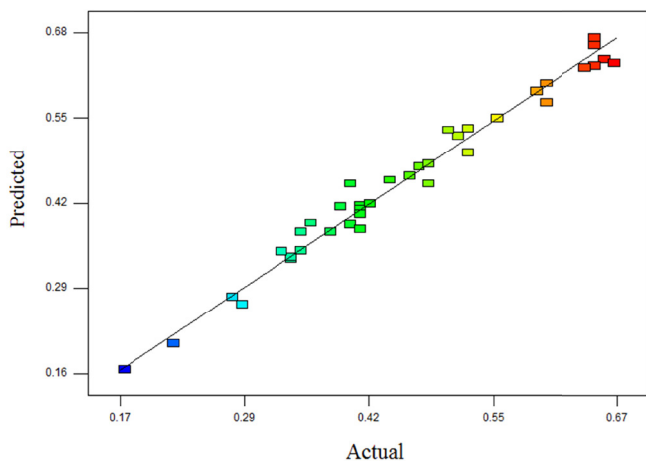


Fig. 5. Predicted vs. actual plot of *DF*.

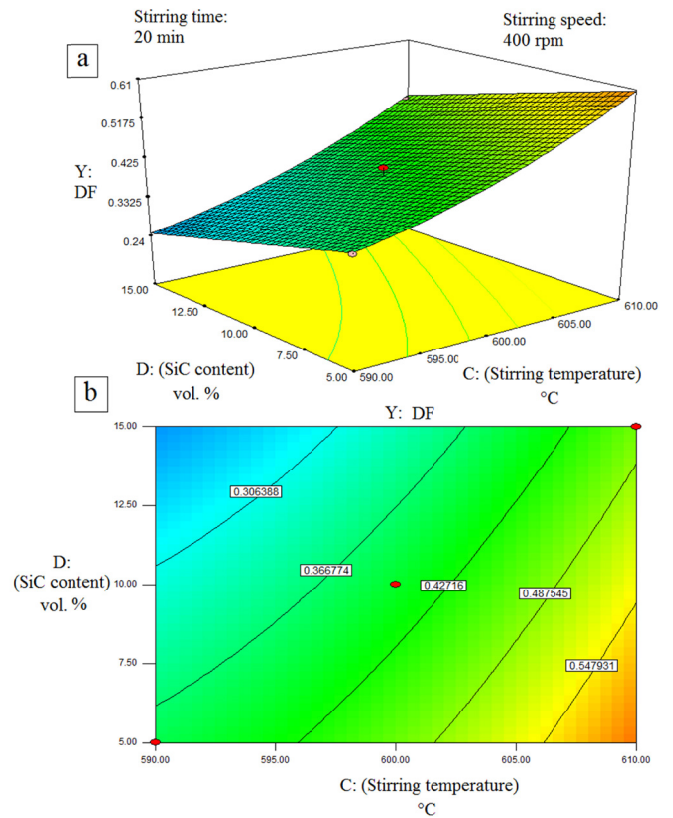


Fig. 4. a) Response surface and b) contour plots for the effect of the stirring temperature and SiC content on the *DF*.

The normality of the data can be checked by plotting a normal probability plot of the residuals. If the data points on the plot fall fairly close to a straight line, then the data are normally distributed [21]. The normal probability plot of the residuals for SF (not shown here) depicted that the data points were fairly close to the straight line and this indicates that the experiments come from a normally distributed population.

The confirmation experiments were conducted in three different conditions. The results are listed in Table 5. If the average of the results of the confirmation is within the limits of the CI, then the significant factors as well as the appropriate levels for obtaining the desired results are properly chosen [17-21]. From Table 5, the experimental responses are in 95% CI range and this model can be used to navigate within the design space.

In order to test the validity of the optimized conditions given by the model, an experiment was also carried out with parameters as suggested by the model. The conditions used in the confirmatory experiment are given in Table 6. The *DF* value at the optimal condition was found to be 0.16 (Table 6), which is consistent with the model. Therefore, the formulated model is acceptably valid. It should be noted that the smaller value of *DF*

Table 5. Results of confirmation tests.

		Stirring speed (rpm)	Stirring time (min)	Stirring temperature (°C)	SiC content (vol. %)	<i>DF</i>
1	Model	400	20	590	10	0.30
	Confirmation test					0.32
2	Model	200	30	600	5	0.51
	Confirmation test					0.53
3	Model	400	20	610	10	0.53
	Confirmation test					0.52

Table 6. *DF* at optimal conditions.

Parameter	Stirring speed	Stirring time	Stirring temperature	SiC content	<i>DF</i>
Model	500 rpm	30 min	590 °C	15 vol %	0.16
Confirmation test					0.19

is indicative of the more uniform distribution of the SiC particles in the matrix [11]. Figure 6 demonstrates the optical micrographs of the composite samples fabricated by different compocasting process parameters and SiC contents for confirmation and optimal condition tests.

Figure 3 shows that *DF* of the SiC particles decreases with increasing the semisolid stirring time, representing a more homogenous SiC distribution within the matrix. At lower stirring time (10 min), in some zones the matrix is free from SiC particles and in other regions clustering of the SiC particles is visible. This shows that this stirring time is insufficient for obtaining an

acceptable SiC distribution in the matrix. Higher stirring time results in a better distribution of the particles. From Figure 4, it can be seen that decreased stirring temperature resulted in a more homogeneous distribution of these particles within the matrix, as indicated by smaller *DF* values. This means that by increasing the semisolid stirring temperature, a less homogeneous distribution of the SiC particles is obtained in the matrix alloy. Decreasing the stirring temperature from 610 to 590 °C (at the fixed stirring speed and stirring time of 400 rpm and 20 min, respectively) leads to a 45% decrease in the *DF* value, which is attributed to the increased viscosity of the semisolid slurry. According to the equilibrium binary Al-Si diagram, A356 aluminium alloy solidifies at a broad temperature interval (32 °C) between 583 to 615 °C. This alloy consists of 45%, 35% and 18% solid fractions in semisolid slurry at 590, 600 and 610 °C, respectively [28]. This shows that the viscosity of the alloy increases as the semisolid temperature decreases. The restricted movement of the particles within the slurry during semisolid stirring prevents the SiC particles from settling as a consequence of the increased effective viscosity; consequently, a more uniform particle distribution is obtained. The presence of a solid phase in the semisolid slurry can also help the breakdown of the SiC clusters during stirring.

The results of this study show a remarkable improvement in the uniformity of the SiC particle distribution (as reflected by the decreased *DF*) when the stirring speed of 500 rpm was used (Figure 3 and Table 6). Particle clustering is observable at a relatively

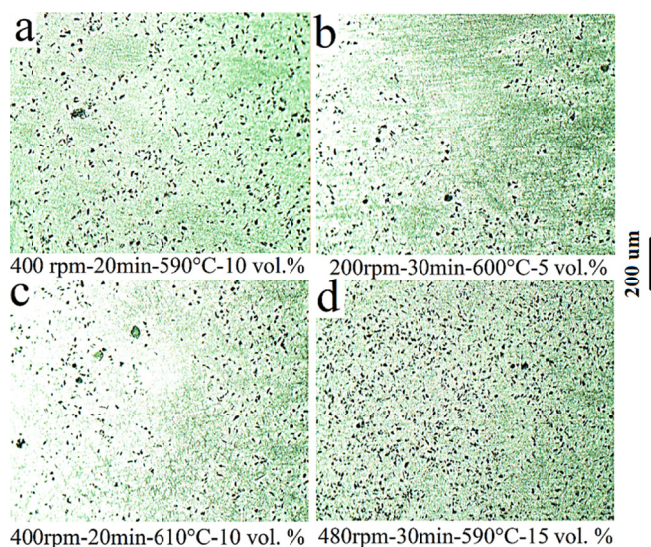


Fig. 6. Optical micrographs of the A356-SiC_p composites fabricated by the different compocasting process parameters and SiC contents (a-c) confirmation tests and (d) at optimal condition.

low stirring speed (i.e. 200 rpm), and in some regions the matrix is free of SiC particles (Figure 6b). By increasing the stirring speed to 500 rpm, a better distribution of the SiC particles within the matrix alloy is obtainable. These results are in agreement with some related studies [10,12], and can be attributed to the increase of shear forces applied by increasing the stirring speed, which can improve the uniformity of the SiC particle distribution as a result of a larger vortex within the slurry. On the other hand, the higher stirring speed (from 500 to 600 rpm) imposed a considerable non-uniformity in the SiC particle distribution, which can be attributed to the increased agitation severity of the slurry, resulting in clustering of the SiC particles.

The effect of the SiC content on the uniformity of the particles distribution within the matrix is given in Figure 4. From this figure, improvement in the uniformity of the SiC particle distribution is obtainable when the particle content increases. This can be attributed to the (a) restricted movement of particles within the melt during solidification as a consequence of the increased effective viscosity of the slurry and (b) finer matrix microstructure as a result of increased barriers for growth of α -Al phase.

4. Conclusion

Compcasting processing of Al-A356-SiC_p composites was studied and modeled using the D-optimal design of experiment (DODE). The effects of compocasting process parameters (stirring temperature, stirring time and stirring speed) as well as SiC content on the uniformity in the particle distribution were investigated. The conclusions drawn from the results can be summarized as follows:

1. The optimum values of stirring temperature, stirring time and stirring speed were found to be 590 °C, 30 min and 500 rpm, respectively.
2. The correlation coefficient (R^2) of the regression model was 0.97, which confirms the excellent accuracy of the model.
3. The most important factor affecting the SiC distribution within the matrix alloy was found to be the stirring temperature.
4. The uniformity in the SiC distribution improved by increasing the SiC content and stirring time and decreasing the stirring temperature. A remarkable improvement in the uniformity of the SiC particle

distribution was achieved when the stirring speed of 500 rpm was used.

References

- [1] N. Chawla, K. K. Chawla, Metal matrix composites, Springer, New York, 2006.
- [2] H. Beygi, M. Shaterian, E. Tohidlou, M.R. Rahimpour, Development in wear resistance of Fe-0.7Cr-0.8Mn milling balls through in situ reinforcing with low weight percent TiC, Adv. Mat. Res. 413 (2012) 262-269.
- [3] B.K. Vinoth, J.J.T. Winowlin, T.P.D. Rajan, M. Uthayakumar, Dry sliding wear studies on SiC reinforced functionally graded aluminium matrix composites, Proceedings of the Institution of Mechanical Engineers, Part L: J. Mater. Design Appl. 30 (2016) 182-189.
- [4] O. El-Kady, A. Fathy, Effect of SiC particle size on the physical and mechanical properties of extruded Al matrix nanocomposites, Mater. Design, 54 (2014) 348-353.
- [5] H. Khosravi, F. Akhlaghi, Comparison of microstructure and wear resistance of A356-SiC_p composites processed via compocasting and vibrating cooling slope, T. Nonferr. Metal. Soc. 25 (2015) 2490-2498.
- [6] S.T. Kumaran, M. Uthayakumar, S. Aravindan, S. Rajesh, Dry sliding wear behavior of SiC and B4C-reinforced AA6351 metal matrix composite produced by stir casting process. Proceedings of the Institution of Mechanical Engineers, Part L: J. Mater. Design Appl. 230 (2016) 484-491.
- [7] S.A. Sajjadi, H. R. Ezatpour, M. Torabi Parizi, Comparison of microstructure and mechanical properties of A356 aluminium alloy/Al₂O₃ composites fabricated by stir and compo-casting processes, Mater. Design, 34 (2012) 106-111.
- [8] B. Abbasipour, B. Niroumand, M. Monir-Vaghefis, Compocasting of A356-CNT composite, T. Nonferr. Metal. Soc. 20 (2010) 1561-1566.
- [9] K.H.W. Seah, S.C. Sharma, M. Krishna, Mechanical properties and fracture mechanism of ZA-27/TiO₂ particulate metal matrix composites, Proceedings of the Institution of Mechanical Engineers, Part L: J. Mater. Design Appl. 217 (2003) 201-206.
- [10] H. Zhang, L. Geng, L. Guan, L. Huang, Effects of SiC particle pretreatment and stirring parameters on

- the microstructure and mechanical properties of SiC_p/Al-6.8Mg composites fabricated by semi-solid stirring technique, *Mat. Sci. Eng. A - Struct.* 528 (2010) 513-518.
- [11] F Akhlaghi, A. Lajevardi, H. M. Maghanaki, Effects of casting temperature on the microstructure and wear resistance of compocast A356/SiC_p composites: a comparison between *SS* and *SL* routes, *J. Mater. Process. Tech.* 155-156 (2004) 1874-1880.
- [12] S.A. Sajjadi, M. Torabi-Parizi, H.R. Ezatpour, A. Sedghi, Fabrication of A356 composite reinforced with micro and nano Al₂O₃ particles by a developed compocasting method and study of its properties, *J. Alloy. Compd.* 511 (2012) 226-231.
- [13] A. Ourdjini, K. Chew, C. Khoo, Settling of silicon carbide particles in cast metal matrix composites, *J. Mater. Process. Tech.* 116 (2001) 72-76.
- [14] L. V. Vugt, L. Froyen, Gravity and temperature effects on particle distribution in Al-Si/SiC_p composites, *J. Mater. Process. Tech.* 104 (2000) 133-144.
- [15] M. Gupta, L. Lu, S. E. Ang, Effect of microstructural features on the aging behavior of Al-Cu/SiC metal matrix composites processed using casting and rheocasting routes, *J. Mater. Sci.* 32 (1997) 1261-1267.
- [16] A. Cetin, A. Kalkanli, Effect of solidification rate on spatial distribution of SiC particles in A356 alloy composites, *J. Mater. Process. Tech.* 205 (2008) 1-8.
- [17] M. J. Anderson, P. J. Whitcomb, *DOE simplified: practical tools for effective experimentation*, New York, Productivity Inc., 2000.
- [18] Software helps Design-Expert Software, Version 7.1, User's guide, Technical Manual, Stat-Ease Inc., Minneapolis, 2007.
- [19] J. Antony, *Design of experiments for engineers and scientists*, Oxford, Heinemann, 2003.
- [20] D.C. Montgomery, *Design and analysis of experiment*, Wiley, New York, 1997.
- [21] A. Dean, D. Voss, *Design and analysis of experiments*, Springer text in statistics, Springer-Verlag, New York, 1999.
- [22] A.K. Sahoo, S. Pradhan, Modeling and optimization of Al/SiC_p MMC machining using Taguchi approach, *Measurement*, 46 (2013) 3064-3072.
- [23] N. Mandal, B. Doloi, B. Mondal, R. Das, Optimization of flank wear using Zirconia Toughened Alumina (ZTA) cutting tool: Taguchi method and regression analysis, *Measurement*, 44 (2011) 2149-2155.
- [24] H. Khosravi, R. Eslami-Farsani, M. Askari-Paykani, Modeling and optimization of cooling slope process parameters for semi-solid casting of A356 Al alloy, *T. Nonferr. Metal. Soc.* 24 (2014) 961-968.
- [25] B. Rahimi, H. Khosravi, M. Haddad-Sabzevar, Microstructural characteristics and mechanical properties of Al-2024 alloy processed via a rheocasting route, *Int. J. Min. Met. Mater.* 22 (2015) 1-9.
- [26] R. Rahmani, F. Akhlaghi, Effect of extrusion temperature on the microstructure and porosity of A356-SiC_p composites, *J. Mater. Process. Tech.* 187-188 (2007) 433-436.
- [27] S. Neseli, S. Yaldiz, E. Turkes, Optimization of tool geometry parameters for turning operations based on the response surface methodology, *Measurement*, 44 (2011) 580-587.
- [28] H. Khosravi, H. Bakhshi, E. Salahinejad, Effects of compocasting process parameters on microstructural characteristics and tensile properties of A356-SiC_p composites, *T. Nonferr. Metal. Soc.* 24 (2014) 2482-2488.